Electrospun boronic acid-containing polymer membranes as fluorescent sensors for bacteria detection

Please, cite as follows:

Jennifer Quirós, Adérito J.R. Amaral, George Pasparakis, Gareth R. Williams, Roberto Rosal, Electrospun boronic acid-containing polymer membranes as fluorescent sensors for bacteria detection, In Reactive and Functional Polymers, Volume 121, 2017, Pages 23-31, ISSN 1381-5148, https://doi.org/10.1016/j.reactfunctpolym.2017.10.007.

Keywords: Boronic acid copolymers; Nanofibres; Electrospun membranes; Biosensor; Bacterial biofilms

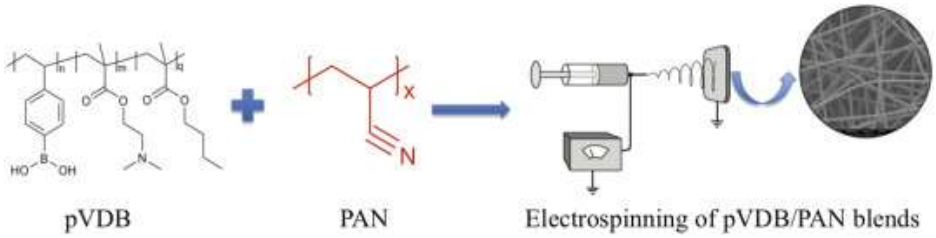

Electrospun boronic acid-containing polymer membranes as fluorescent sensors for bacteria detection

JenniferQuirós[1,2,*], Adérito J.R. Amaral[2], George Pasparakis[2], Gareth R. Williams[2], RobertoRosal[1]

[1] Department of Chemical Engineering, University of Alcalá, 28871 Alcalá de Henares, Madrid, Spain

[2] UCL School of Pharmacy, University College London, 29-39 Brunswick Square, London WC1N 1AX, UK

* Corresponding author: jennifer.quiros@uah.es

Abstract

In this work, a boronic acid copolymer, poly(4-vinylphenylboronic acid-co-2-(dimethylamino)ethyl methacrylate-co-n-butyl methacrylate) (pVDB) was designed for the rapid detection of bacteria based on reversible boronate ester formation with the diol-rich saccharide moieties found on bacterial membranes. Electrospun nanofibre membranes were prepared from a blend of polyacrylonitrile (PAN) and pVDB, which was synthesized by free radical polymerization. The pVDB@PAN membranes were used as fluorescent bacterial biosensors, displaying a distinct emission at 538 nm when in contact with bacteria cells. The fluorescence intensity showed a maximum intensity after 24 h of contact with *Staphylococcus aureus* or *Escherichia coli*, and this intensity increased proportionally with the pVDB content in the electrospun membranes. When in contact with *Pseudomonas putida*, the membranes became non-responsive within 8 h due to the rapid formation of a bacterial biofilm. This fouling phenomena blocked the membrane surface for fluorescence readings. The pVDB@PAN biosensor allowed for the rapid detection of the early stages of bacterial colonization well before biofilm formation, which could be advantageous for the early identification of pathogenic bacteria and prevention of their spreading.

Keywords: Keywords: Boronic acid copolymers; Nanofibres; Electrospun membranes; Biosensor; Bacterial biofilms

1. Introduction

Infectious diseases are still among the leading causes of death worldwide, despite numerous advances in medical research [1]. The increasing global spread of antibiotic resistant bacteria, and the prevalence of nosocomial infections, cause increased morbidity and mortality in patients and constitute a serious problem for public health [2]. New antibiotic resistance mechanisms are constantly emerging and compromise our ability to treat even common infectious diseases, which results in prolonged illness, disability, and ultimately death. For example, resistance of *E. coli* to fluoroquinolone antibiotics, among the most widely used and highest potency medicines for the treatment of urinary tract infections, is already widespread; there are currently parts of the world where treatment is virtually ineffective in more than half of patients [3].

The establishment of bacterial infections involves several mechanisms, which require the initial adhesion of pathogenic bacteria to host cells (through the action of specific lectin-carbohydrate interaction motifs), followed by colonization and biofilm formation at the site of infection [4–6]. Several pathogens associated with chronic infections are linked to biofilm formation, including those causing periodontitis, cystic fibrosis, pneumonia, chronic urinary tract infections, chronic otitis media, and chronic wound infections [7]. Chronic infections arise in part because bacteria in biofilms can effectively resist the host immune response as well as antibiotic treatment, which imparts them with the ability to persist for a long time in the human body [8].

In recent years, boronic acid (BA) derivatives have attracted significant interest in cell capture and release technologies, as well as in carbohydrate sensing, owing to their ability to form covalent (albeit reversible) complexes with *cis*-diol residues. These are abundant on the surface of bacterial cells due to their carbohydrate-rich compositions [9,10]. A range of design concepts comprising boronic acids have been recently reported for the detection and quantification of diol-rich carbohydrates or bacterial cells; these include the coupling of boronic acids with fluorescent tags [11–15], immobilization on electrodes, or their chemical immobilization on the surfaces of bioelectronic devices [16,17].

In this work, we explored electrospinning as an effective method to incorporate boronic acids in fluorescent polymeric nanofibres. Electrospinning is an extremely versatile technique to prepare submicron fibrous membranes from a wide variety of polymers and blends either dissolved in organic or aqueous media, or in their melt form [18]. We report the use of nanofibrous membranes prepared from a blend of polyacrylonitrile, which serves as a fluorescent reporter tag, and a boronic acid-based copolymer for the capture of bacterial cells. Electrospinning allows the deposition of nanofibres in the form of thin membranes that exhibit very high surface area to volume ratios, providing abundant opportunities for contact with

bacteria. The presence of BA in the fibres should facilitate robust binding with both gram-positive and gram-negative bacteria. Thus, the systems prepared here will have the ability to bind effectively with bacteria, and the presence of a fluorescent reporter tag will provide a convenient readout of binding. A schematic of our experimental approach is given in Scheme 1. To the best of our knowledge, this is the first time a boronic acid-based membrane composed of polymeric nanofibres has been used as a biosensor for the detection of bacteria.

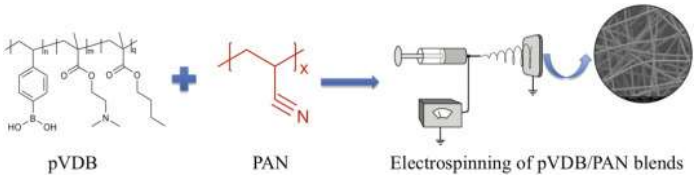

Scheme 1. An outline of the experimental approach taken in this work.

2. Experimental

2.1. Materials

Polyacrylonitrile (PAN, average MW 150,000), 4-vinylphenylboronic acid (98%, VPBA), *n*-butyl methacrylate (99%, BUMA), 2,2′-azobis(2-methylpropionitrile) (AIBN), 2-(dimethylamino)ethyl methacrylate (DMAEMA), dimethyl sulfoxide (DMSO), ethanol (96%), *N,N*-dimethylformamide (DMF), *N,N*-dimethylacetamide (DMAc) and hexane were purchased from Sigma Aldrich. Culture media components comprised beef and yeast extract and soy peptone (purchased from Pronadisa-Conda, Spain), and sodium chloride (sourced from Panreac). FilmTracer™ *SYPRO® Ruby Biofilm Matrix Stain* was obtained from Thermo Fisher-Invitrogen.

2.2. Synthesis of pVDB

The polymer was synthesized by modifying previously published protocols [19–21]. In a 50 mL round-bottom flask, VPBA (104 mg, 0.7 mmol), DMAEMA (110 mg, 0.7 mmol) and BUMA (2 g, 14 mmol) at molar ratios 5:5:90 were dissolved in 7 mL of a DMSO:ethanol (1:1, v/v) mixture. AIBN (25 mg, 0.15 mmol) was added to the flask, which was then sealed before purging with argon for 5–10 min. The reaction mixture was placed in an oil bath at 75 °C for 24 h under magnetic stirring. The polymer was recovered by precipitation in hexane and dried under vacuum. The copolymer was isolated as a pale yellow solid (yield 70%).

2.3. Electrospinning

Electrospun fibres were prepared by dissolving 30 wt% of pVDB polymer in DMAc under constant magnetic stirring for 6 h. Subsequently, this solution was mixed at different ratios with a 10 wt% solution of PAN in DMF (see Table 1). After vigorous magnetic stirring for 24 h, the resulting dispersion was transferred to a 5 mL syringe fitted with a 21-gauge stainless steel blunt-tip needle. The needle was in turn connected to a high voltage power supply (HCP35–35,000, FuG Elektronik). A syringe pump (KDS100, Cole-Parmer) and a flat collector plate (16 × 16 cm, covered in aluminium foil) completed the assembly. All processes were conducted under ambient conditions (22 ± 3 °C, and 40 ± 5% relative humidity) at a flow rate of 0.5 mL/h, with a 24 cm distance between the needle and the collector. The applied voltage was 18 kV, with the exception of pVDB60@PAN which was prepared at 21 kV. The fibre formulations and electrospinning parameters are described in Table 1.

2.4. Analytical methods

^{1}H NMR spectra were recorded with deuterated chloroform ($CDCl_3$) as an internal standard using a Bruker DRX 400 MHz spectrometer. The morphology and the diameter of the electrospun nanofibres were analysed with scanning electron microscopy (SEM, FEI Quanta 200 FEG-SEM instrument) after sputtering the samples with a 20 nm gold layer. The average fibre diameter for each sample was calculated by measuring around 100 fibres in the SEM images using the ImageJ software (National Institutes of Health, USA). Fourier transform infrared spectroscopy (FT-IR) was conducted using a Nicolet-Nexus 670 FT-IR spectrometer over the range 650–4000 cm^{-1}, with a resolution of 2 cm^{-1}.

The surface ζ-potential of the fibres was measured using electrophoretic light scattering (Malvern Zetasizer Nano ZS instrument) with the aid of the appropriate Malvern surface zeta potential cell (ZEN 1020). In brief, a rectangular section not larger than 7 mm × 4 mm was glued onto the sample holder using Araldite adhesive. The cell was inserted into a disposable plastic 10 mm square cuvette containing 1.2 mL of 10 mM aqueous KCl (with pH adjusted to

Table 1. Details of the fibre formulations, including electrospinning parameters, surface ζ-potential, water contact angle and fibre diameter. All processes were conducted under ambient conditions (22 ± 3 °C, and 40 ± 5% relative humidity) at a flow rate of 0.5 mL/h, with a 24 cm distance between the needle and the collector.

ID Sample	Polymer	Polymer in fibres (% w/w)	Voltage (kV)	Surface ζ-potential (mV)[a]	Water contact angle (°)	Fibre diameter (nm)
PAN	PLA	100	18	-1.3 ± 0.9	-	497 ± 67
pVDB40@PAN	PAN/pVDB	60/10	18	-1.5 ± 0.4	120 ± 15	553 ± 141
pVDB50@PAN	PAN/pVDB	50/50	18	-4.8 ± 0.5	134 ± 3	592 ± 70
pVDB60@PAN	PAN/pVDB	40/60	21	-7.0 ± 1.2	143 ± 10	559 ± 112

[a] pH 7.0

7.0 prior to measurements, using 1 M KOH and 1 M HCl), with 0.5% (w/w) polyacrylic acid (450 kDa) as a tracer (a negatively charged tracer is required for negatively charged surfaces). Measurements were performed at 25 °C at six different distances from the sample surface, which enabled the surface zeta potential to be calculated by the Zetasizer software. Membrane wettability was tested on an optical contact angle meter (Krüss DSA25 Drop Shape Analysis System) at room temperature, using the sessile drop technique. A fluorescence spectrophotometer (Varian Cary Eclipse) was used for recording the fluorescence spectra of the pVDB-based membranes. During the emission scan, the excitation monochromator was set to a fixed wavelength and the emission monochromator scanned over a wavelength range (200 nm greater that the emission scan value). The excitation was varied from 250 nm to 645 nm at 10 nm intervals.

2.4. Bacterial assays

The microorganisms used in this study were *Escherichia coli* (ATCC 8739), *Pseudomonas putida* (DSMZ 84) and *Staphylococcus aureus (*ATCC 6538P). Cultures were grown overnight in nutrient broth under moderate shaking. The broth comprised (for 1 L in distilled water): 1 g beef extract, 2 g yeast extract, 5 g peptone, 5 g NaCl, and the pH was adjusted to 7.2. After reactivation, the cell density was tracked by measuring the optical density at 600 nm (OD_{600}). Exponentially growing cultures on nutrient medium were diluted to an OD_{600} of 0.0138 for *P. putida* and *E. coli* and 0.0400 for *S. aureus*. 1 mL aliquots were placed on circular pVDB@PAN samples (15 mm diameter) inside 24-well polystyrene plates and incubated without shaking at 28 °C (*P. putida*) or 30 °C (*S. aureus*, *E. coli*).

The biosensor capacity of the pVDB-containing membranes was studied by following in parallel the autofluorescence emitted by the membranes in contact with bacteria, and the colonization behaviour of these three strains on the membrane surface in specific time frame, including 8, 24 and 48 h.

For the visualization of biofilms after incubation, the liquid culture was removed, and the membranes carefully rinsed with distilled water before being stained with 100 µL FilmTracer SYPRO Ruby Biofilm Stain (Molecular Probes, Thermo Fisher Scientific). Stained membranes were incubated in the dark for 30 min at room temperature, and then rinsed with distilled water. The specimens were transferred to a glass slide, covered with a glass cover slip, and sealed. All images were recorded at 24 and 48 h after inoculation using a SP5 confocal fluorescence microscope (Leica Microsystems) at excitation/emission wavelengths of 450/610 nm. Images of bacteria colonizing the surface of materials were recorded on a Hitachi TM-1000 microscope. For this, a process of cell fixation in glutaraldehyde 5% (v/v) in 0.2 M sodium cacodylate buffer pH 7.2 was first carried out for 1 h at room temperature. Samples were then rinsed in cacodylate buffer and dehydrated in an ascending ethanol series (25, 50, 70, 90 and 100%) before critical point drying with CO_2 and subsequent observation with SEM. The fluorescence emitted by the pVBD@PAN membranes in contact with bacteria was measured in a fluorometer/luminometer (Fluoroskan Ascent FL). The wavelength range was fixed according to the data obtained from the fluorescence spectra; excitation was set at 360 nm and emission at 538 nm. 24-well polystyrene plates containing fibre membranes before and after incubation were place inside the Fluoroskan holder. The fluorescence emitted was measured in top-scan mode, using an integration time of 60 ms. This method allowed 31 data points to be obtained for each surface.

An additional experiment was carried out to validate the responsive of pVDB membranes to bacteria attachment after a glucose saturation. 1 mL of a glucose solution (1 g/L) was placed on circular pVDB@PAN samples (15 mm diameter) inside 24-well polystyrene plates at room temperature by 6 h. Prior bacteria contact, the glucose was extracted and then 1 mL aliquots were added on membranes specimens and incubated 24 h without shaking at 28 °C (*P. putida*) or 30 °C (*S. aureus*, *E. coli*).

3. Results and Discussion

3.1. Characterisation of pVDB

The copolymer was first characterized by ^{1}H NMR (Fig. 1). The spectrum is fully consistent with the formation of the desired polymer, with characteristic aromatics peaks of PBA visible at ca. 7.1-7.6 ppm.

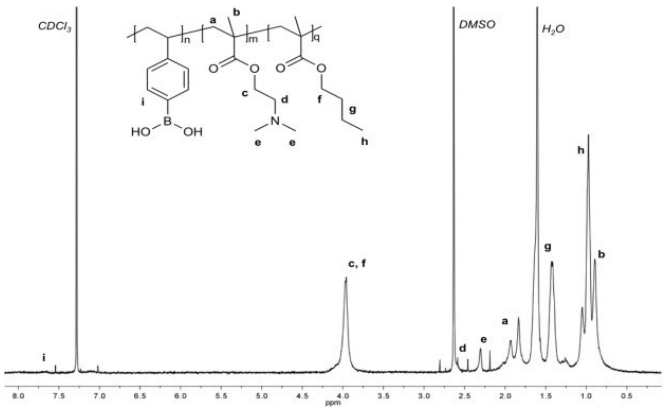

Figure 1. ^{1}H NMR spectrum of the pVDB in $CDCl_3$.

Fig. 2a shows the FT-IR spectrum of the synthesized pVDB polymer. The spectrum is dominated by a strong band at ~ 1730 cm^{-1} due to the C=O stretching of the methacrylate ester group. Minor bands correspond to stretching modes of the methyl group at 2940 cm^{-1}, together with bands of the dimethylamino group from the DMAEMA component at 2819 and 2767 cm^{-1}[22]. Signatures of the phenyl boronic moieties can be seen at 1430 cm^{-1} (due to the combined motions of the C-C stretch of the aromatic ring and the B-O stretch),

1340 cm^{-1} (vibrational modes involving B-O stretching), 1100 cm^{-1} (phenyl ring deformation) and the broad mode centred at 3300 cm^{-1} (O-H stretching motions of the -$B(OH)_2$ moiety, which likely overlaps with vibrational bands from water molecules trapped in the sample [23]. The IR spectrum is thus consistent with the production of the desired copolymer.

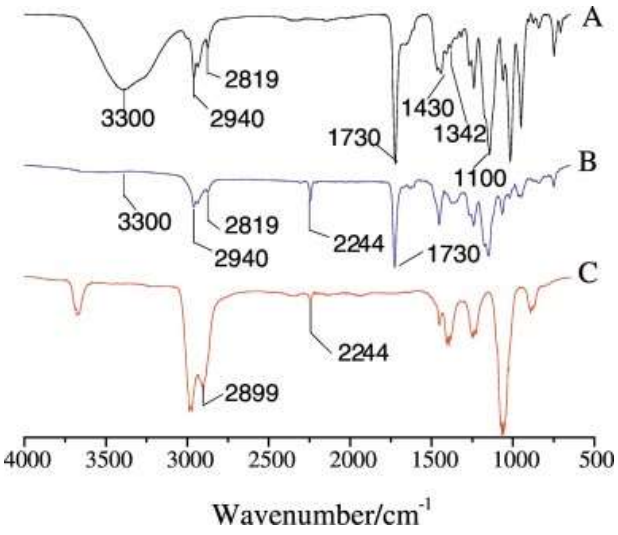

Figure 2. FT-IR spectra of (A) pVDB, (B) pVDB60@PAN, and (C) PAN.

3.2. Characterisation of the electrospun fibres

The spectrum of pure PAN fibres (Fig. 2) shows bands at 2899 cm^{-1} (− CH_2– stretching) and 2244 cm^{-1} (−CN). That of the pVDB60@PAN blend membrane shows absorption bands of both the pVDB (at approximately 2940 cm^{-1}, 2819 cm^{-1}, 1730 cm^{-1}) and of PAN (at ca. 2244 cm^{-1}). It is clear that both polymers are incorporated into the fibres without any loss of structural integrity.

Fig. 3 depicts representative SEM micrographs of the nanofibre membranes formed using PAN/pVDB polymer blends containing different feed ratios of the pVDB polymer. The morphology and diameter of the electrospun fibres depend on a number of parameters including the applied voltage, the electrospinning distance, and the solution concentration [24]. Most of the fibres were linear and cylindrical in shape. The average diameter of the fibres did not change significantly with increasing the pVDB concentration, and in all cases lies in the 500–600 nm range (Table 1). However, it was observed that at 60 wt% pVDB and 18 kV voltage, the electrospinning process became unstable, leading to ill-defined fibres, and it was necessary to increase the voltage to 21 kV in order to obtain uniform beadless fibres (as shown in Fig. 3D).

Membrane hydrophilicity is an important factor that influences the attachment of microbial cells to surfaces [25]. We studied this by measuring the water contact angles for all the electrospun membranes, as given in Table 1.

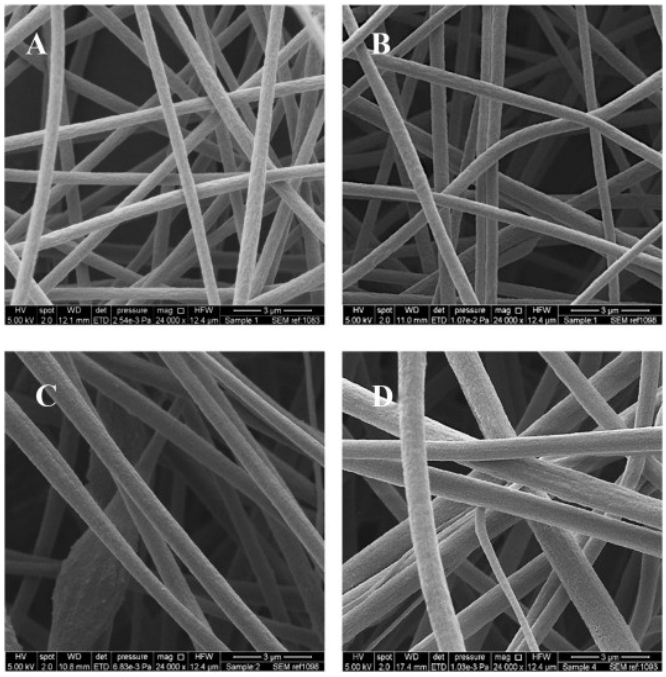

Figure 3. SEM micrographs of nanofibres prepared with different ratios of PAN: pVDB (compositions are given in Table 1). (A) PAN (B) pVDB40@PAN (C) pVDB50@PAN and (D) pVDB60@PAN. Scale bar: 3 μm.

Water droplets deposited on the PAN membranes rapidly spread across the membrane surface, exhibiting a superhydrophilic behaviour consistent with the texture of a nanofibrous surface made up of a hydrophilic polymer [26]. Conversely, the pVDB-containing fibres displayed hydrophobic contact angles that increased from 120 ± 15° to 143 ± 10° as the pVDB content rose from 40 to 60 wt% (Table 1).

The ζ-potentials of the electrospun membranes are also listed in Table 1. All were negatively charged, with surface charge becoming more negative as the concentration of pVDB in the fibres increased. This is expected because DMAEMA is protonated at pH 7.0, whereas the boronic acid should exist in the tetrahedral form and be negatively charged, and hence the overall zeta potential should be negative for these fibres [12].

The fluorescence spectra of the pVDB@PAN electrospun membranes showed different emission bands when the excitation wavelength was set at 255 nm, 385 nm and 505 nm. Upon excitation at 255 nm, two peaks were observed in the 265–465 nm emission range (at 298 nm and 428 nm) (Supplementary Data, Fig. S1). Exciting at 385 nm, three peaks were obtained in the 395–595 nm emission range at 429, 485 and 528 nm (Fig. 4). Finally, at excitation wavelength of 505 nm two main peaks appeared at 528 and 543 nm) (Fig. S2). These results were used as a reference to set the excitation/emission wavelengths for the biosensing assays. It was observed that exciting the pVDB@PAN membranes in contact with bacteria at 360 nm resulted in a clear signal at 538 nm, which corresponded with the peak obtained in the fluorescence spectrum when exciting at 385 nm (Fig. 4).

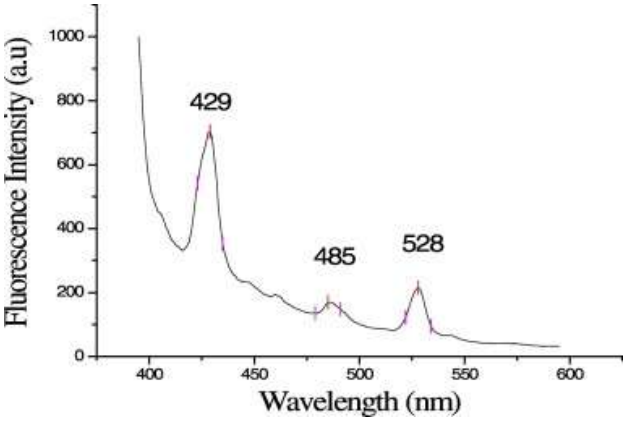

Figure 4. The fluorescence spectrum of pVDB60@PAN (λ_{ex} = 385 nm).

3.3. Microbial colonization of electrospun membranes

The pure PAN fibres were considerably more resistant to bacterial colonization than the pVDB-containing fibres. This is clearly shown in the SEM images of membranes exposed for 8 and 24 h (Fig. 5), and 48 h (Fig. S3) to cultures of *E. coli*, *P. putida* and *S. aureus*. The images also demonstrate that the PAN membranes are essentially free of *E. coli* cells even after 48 h. *P. putida* and *S. aureus* led to a certain degree of colonization, but without developing biofilms. Conversely, the pVDB-containing fibres displayed extensive bacterial colonization and clear biofilm formation.

Electrostatic interactions have been shown to play a role in microbial adhesion, either attracting or repelling the outer membranes of bacterial cells, which bear a negative charge [27]. The ζ-potentials reported for *E. coli* and *S. aureus* are − 44.2 and − 35.6 mV respectively [28], while Neumann and co-workers reported − 14 mV as the ζ-potential of *P. putida* [28,29]. Our data showed that the more negatively charged surfaces (pVDB60@PAN) underwent the greatest extent of bacterial colonization, as revealed by SEM and Ruby FilmTracer micrographs (Figs. 5 and 6 and Fig. S3). In spite of the recognized role of surface charge in the initial stages of bacteria attachment, biofilm formation can also be governed by other factors [30]. The value of the contact angles (Table 1) revealed that the pVDB-containing membranes were superhydrophobic with contact angles of 120° for pVDB40@PAN, 134° for pVDB50@PAN and 143° for pVDB60@PAN. In contrast, the PAN membranes demonstrated extreme hydrophilicity with a measured contact angle of 0°. Therefore, we believe that for these fibres, their superhydrophobicity (possibly in combination with gravitational force), is the dominant factor that governs the initial adhesion of the bacteria to the membranes.

The contact angle values are dependent on chemical composition, porosity, and surface roughness [31,32]. In fact, recent experimental results have indicated that the roughness alone can greatly magnify the (de-)wetting properties of a surface even without altering the chemical composition [33]. In order to demonstrate the role of roughness on the wetting properties of the membranes, we measured the contact angle of pVDA polymers in the form of thin films using blends at the same ratios as those of the electrospun fibres. The results showed contact angles considerably smaller compared to the nano-fibrous textured counterparts (Tables 1 and S1). The water contact angles on pVDB-containing films were 83 ± 5° for pVDB40@PAN, 85 ± 3° for pVDB50@PAN and 87 ± 3° for pVDB40@PAN and 56 ± 4° on PAN films, reflecting that the chemical composition of the pVDB significantly contributes to the high contact angle values of the pVDB-containing membranes, which in turn influence biofilm formation. These findings are in accord with previous reports showing that smooth surfaces do not favour bacterial adhesion [31,32]. Therefore, nanofibrous membranes might offer more adhesion points for bacterial anchoring motifs owing to their increased roughness and the larger available surface area for bacterial contact, as a result of their high aspect ratios.

The images shown in Fig. 5 provide some insight into the process of biofilm formation on the membrane surface. The attachment of bacterial cells to the surface takes place via the development of primary micro-colonies that produce a primitive extracellular matrix holding them together. Then, the micro-colonies progressively enlarge and coalesce to form successive layers of cells covering the surface, which eventually lead to a maturity stage with larger macro-colonies surrounded by water channels that help distribute nutrients and signalling molecules [8]. Our images show that the initial steps of biofilm formation on the pVDB-containing fibres occurred before 8 h for *S. aureus* and *E. coli*, while the PAN fibres reached this stage between 24 and 48 h (see Fig. 5). The images of membranes in contact with *P. putida* at 8 h clearly show mature biofilms on the fibre surfaces, while PAN fibres achieved this phase only after 24 h (Fig. 5). This information is supported by confocal micrographs recorded with the use of a Ruby FilmTracer fluorescent probe (Fig. 6), which reveal the protein-rich formation of the bacterial extracellular matrix. This consists of glycoproteins, phosphoproteins, lipoproteins, calcium binding proteins, fibrillar proteins, and other proteins [34]. It should be noted that a typical biofilm exhibits relatively heterogeneous thickness and could contain several undefined components that differ with species and conditions [34]. Nevertheless, our chosen fluorescent probe captured relatively reliably the formation of the biofilms due to its non-specific protein-staining capacity irrespective of the bacterial strain used. As expected, by increasing the contact time, an increase in extracellular matrix formation was observed, indicating extensive biofilm proliferation on the pVDB-containing fibres. On the PAN fibres, however, bacterial spreading was considerably lower,

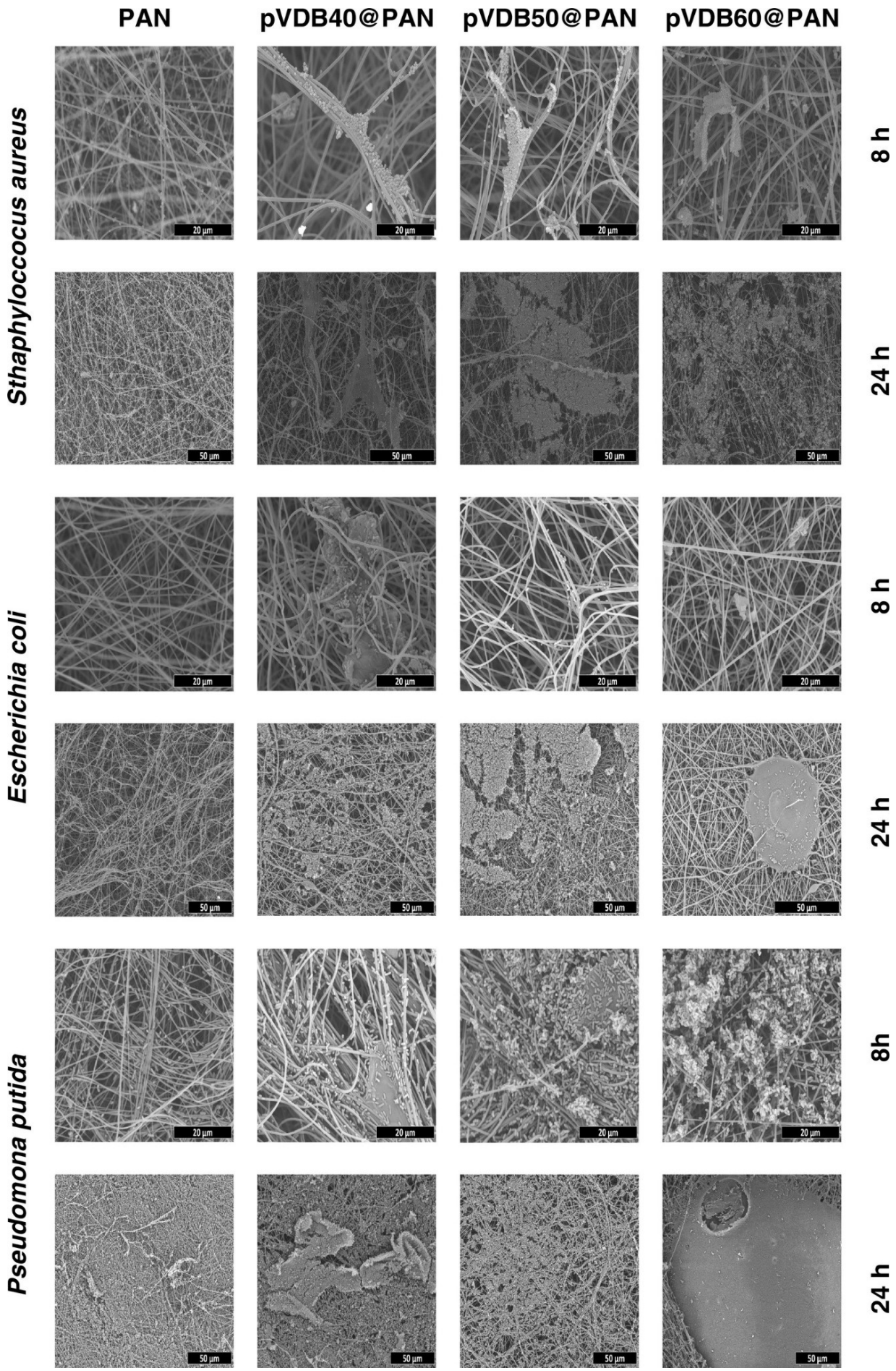

Figure 5. SEM micrographs of PAN, pVDB40@PAN, pVDB50@PAN and pVDB60@PAN membranes after 8 and 24 h of static incubation with *S. aureus* (at 30 °C), *E. coli* (at 30 °C) and *P. putida* (at 28 °C). Scale bars (8h) = 20 µm, Scale bars (24 h) = 50 µm.

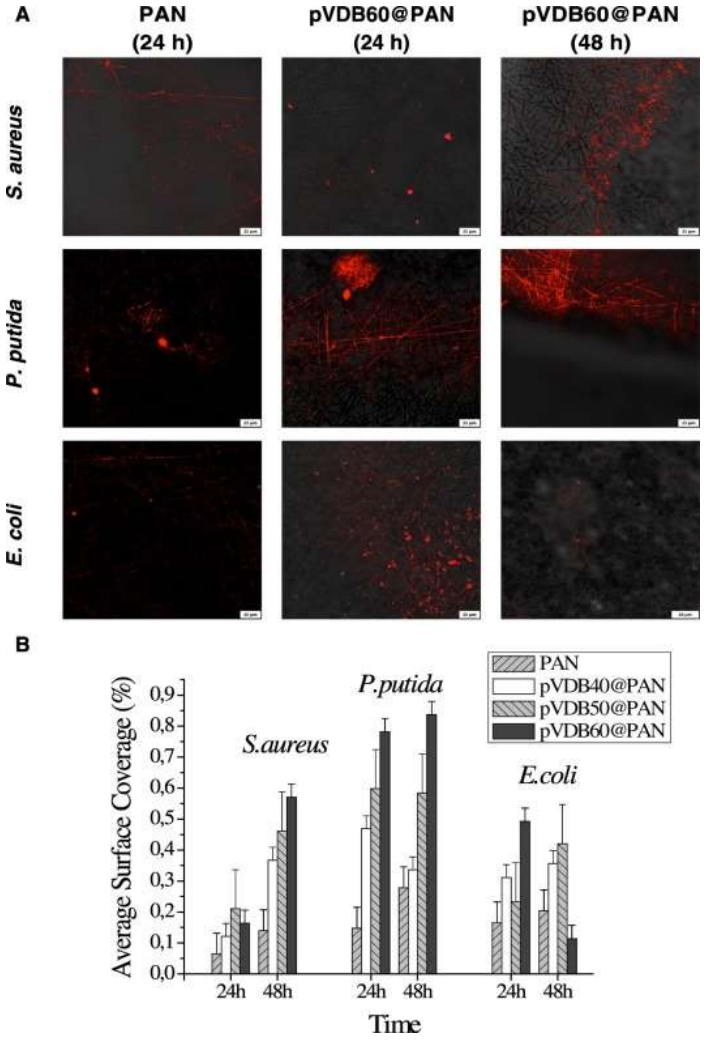

Figure 6. (A) FilmTracer™ SYPRO™ Ruby biofilm matrix staining of PAN and pVDB60@PAN membranes in contact with. S. aureus, E. coli and P. putida cultures for 24 and 48 h. (B) Average surface coverage percentages of biofilm matrices on PAN and pVDB membranes, after 24 and 48 h of static incubation with *S. aureus* (at 30 °C), E. coli (at 30 °C) and *P. putida* (at 28 °C). Surface coverage percentages were calculated using confocal micrographs, with the ImageJ program (n = 131, 3 independent runs). Scale bars = 25 μm.

with reduced biofouling. At 48 h, when the pVDB@PAN membranes develop a mature biofilm, multiple layers of cells accumulate on the surface, as shown by the SEM micrographs (Fig. S3). As a result, some of the extracellular matrix may become covered, which would explain the reduced biofilm surface coverage revealed by the staining of extracellular proteins in the case of *E. coli* after 48 h with pVDB60@PAN (Fig. 6). The results clearly show that the inclusion of the pVDB significantly augments bacterial attachment. This was validated by exposing PAN and pVDB-containing fibres to a saturated glucose solution (1 g/L, 6 h) prior to contact with bacteria culture (Fig. S4). A significant decrease of bacterial adhesion, particularly for *P. putida,* was observed: this is attributed to the fact that free glucose binds to the boronic acid residues of the fibers and blocks potential binding with the diols present on bacterial surfaces. Ultimately, this reduces bacterial attachment and biofilm formation [35]. Therefore, this set of experiments corroborates our hypothesis that the boronic acids on the fibres mediate specific ligand-receptor types of adhesion cascades, acting in concert with non-specific interactions (e.g. hydrophobicity) that drive the attachment of bacterial cells to the membranes.

3.4. Biosensing assays

The biosensing capacity of the pVDB-containing fibres was studied upon contact with all three bacterial strains. Fluorescence readings were recorded at 538 nm with an excitation wavelength at 360 nm. The measurements were performed after the membranes had been in contact with bacteria for 8, 24 and 48 h in microplates. The results are shown in Fig. 7 and are reported as relative fluorescence units (RFU; an RFU of 1 corresponds to the pure PAN control fibres). The results can be interpreted in terms of the ability of pVDB to form reversible covalent complexes with the 1,2-diols and 1,3-diols of bacterial wall carbohydrates [36,37].

The increase in fluorescence observed for pVDB-containing fibres in contact with *E. coli* and *P. putida* can be rationalized due to the binding of pVDB to the bacterial membrane lipopolysaccharides. The cell wall of Gram-negative bacteria is composed of a thin layer of peptidoglycan and an outer membrane with phospholipids and boronic-acid interacting lipopolysaccharides [38]. Conversely, Gram-positive bacterial cell walls are composed of multiple peptidoglycan layers, with a wall of lipoteichoic acids bridging the peptidoglycan and the cytoplasmic membrane. The teichoic acid found in the Gram-positive *S. aureus* is a water-soluble polymer composed of 40 ribitol phosphate units substituted with a D-alanine ester and *N*-acetylglucosaminyl residues. The chain is attached to peptidoglycans by a phosphodiester bond, through a linkage unit that is composed of three glycerophosphate residues linked to two amino sugars; the latter is a diol target for possible pVDB binding [39]. The fluorescence intensity shows a maximum after 24 h contact with *S. aureus* and *E. coli*, with higher intensity upon increasing the concentration of pVDB in the fibres. This effect is even more pronounced in *E. coli*, which can be explained because the Gram-negative *E. coli* presents many free diol groups in its lipopolysaccharides' outer membrane which can bind with boronic acid moieties in the fibre membranes. Gram-positive *S. aureus,* with a reduced number of sugars accessible in the thick peptidoglycan layer, led to moderate fluorescence intensities. In the case of the Gram-negative *P. putida*, however, the membrane rapidly became non-responsive and only the pVDB60@PAN sample displayed appreciable fluorescence after 8 h contact with bacterial cells. These data were consistent with the fouling behaviour shown in Fig. 5, from which it is apparent that *P. putida* develops a mature biofilm after 8 h in contact

with the pVDB@PAN fibres. These mature biofilms could be blocking the membrane surface for fluorescence readings.

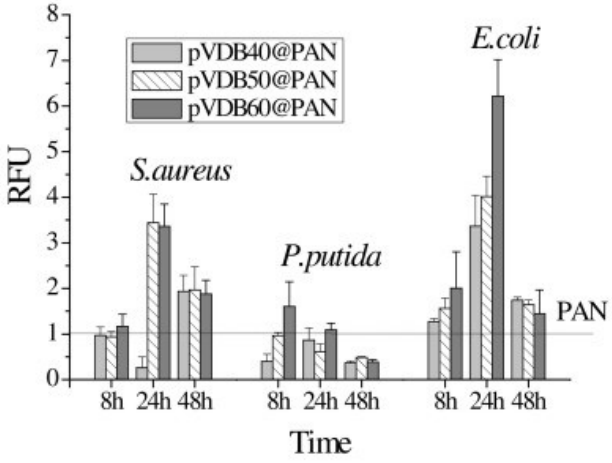

Figure 7. The fluorescence intensity of pVDB-containing fibres after contact with bacteria. $\lambda_{ex.}$ = 360 nm $\lambda_{em.}$ = 538 nm. 6 replicates per membrane and strain, 31 data points were obtained over each surface. The dashed line corresponds to PAN. RFU = relative fluorescence units, and RFU = 1 is for the control PAN membrane without pVDB.

The inclusion of the boronic acid unit into a polymer matrix is a simple way of developing analytical devices, since the polymer imparts many advantages over the free boronic acid complex. These include improved robustness, sensitivity, handling, and biocompatibility, which are important properties for the development of bacterial sensors [40]. This work shows that pVDB containing electrospun membranes provide sensors responsive to bacterial attachment and allowing their early detection, which could be useful to prevent irreversible damage of biomaterials and tissues due to fouling.

4. Conclusions

In summary, our work demonstrates the efficiency of electrospun nanofibrous membranes prepared from a blend of polyacrylonitrile and a boronic acid-based polymer as a fluorescent bacterial biosensor. The morphology and composition of the pVDB@PAN membranes prepared allowed effective bacterial attachment and rapid monitoring via a straightforward fluorescent readout mechanism. The high affinity and specificity of the pVDB-containing membranes towards both Gram-negative and Gram-positive bacteria was demonstrated by the extensive bacterial colonization and biofilm formation observed with three different bacterial strains. The fluorescent response of the pVDB-containing electrospun materials allowed for simple bacterial detection at the early stages of microbial colonization, which could have great potential in the design of bioelectronics and biosensing devices.

Acknowledgements

Financial support for this work was provided by the FP7-ERA-Net Susfood (2014/00153/001), the Spanish Ministry of Economy and Competitiveness (CTM2013-45775-C2-1-R) and the Regional Government of Madrid through program S2013/MAE-2716-REMTAVARES-CM. UCL (UCL Excellence Fellowship, AJRA and GP) and the Leverhulme Trust (ECF-2013-472, GP) are also kindly acknowledged for financial support.

References

[1] Institute of Medicine (US) Forum on Microbial Threats. Microbial Evolution and Co-Adaptation: A Tribute to the Life and Scientific Legacies of Joshua Lederberg: Workshop Summary. The national academies collection: reports funded by national institutes of health, National Academies Press (US) National Academy of Sciences, Washington (DC) (2009)

[2] T.U. Berendonk, et al., Tackling antibiotic resistance: the environmental framework, Nat. Rev. Microbiol., 13 (5) (2015), pp. 310-317

[3] L.S. Redgrave, S.B. Sutton, M.A. Webber, L.J.V. Piddock, Fluoroquinolone resistance: mechanisms, impact on bacteria, and role in evolutionary success, Trends Microbiol., 22 (8) (2014), pp. 438-445

[4] A.M. Krachler, K. Orth, Targeting the bacteria-host interface: strategies in anti-adhesion therapy, Virulence, 4 (4) (2013), pp. 284-294

[5] M. Mammen, S.-K. Choi, G.M. Whitesides, Polyvalent interactions in biological systems: implications for design and use of multivalent ligands and inhibitors, Angew. Chem. Int. Ed., 37 (20) (1998), pp. 2754-2794

[6] S.R. Shames, S.D. Auweter, B.B. Finlay, Co-evolution and exploitation of host cell signaling pathways by bacterial pathogens, Int. J. Biochem. Cell Biol., 41 (2) (2009), pp. 380-389

[7] W. H. Organization, Critically important antimicrobials for human Medicine (2017)

[8] D. Dufour, V. Leung, C.M. Lévesque, Bacterial biofilm: structure, function, and antimicrobial resistance, Endod. Top., 22 (1) (2010), pp. 2-16

[9] G. Vancoillie, R. Hoogenboom, Synthesis and polymerization of boronic acid containing monomers.,Polym. Chem., 7 (35) (2016), pp. 5484-5495

[10] N.D. Winblade, I.D. Nikolic, A.S. Hoffman, J.A. Hubbell, Blocking adhesion to cell and tissue surfaces by the chemisorption of a poly-l-lysine-graft-(poly(ethylene glycol); phenylboronic acid) copolymer, Biomacromolecules, 1 (4) (2000), pp. 523-533

[11] G. Pasparakis, A. Cockayne, C. Alexander, Control of bacterial aggregation by thermoresponsive glycopolymers, J. Am. Chem. Soc., 129 (36) (2007), pp. 11014-11015

[12] X. Xiong, Z. Wu, Q. Yu, L. Xue, J. Du, H. Chen, Reversible bacterial adhesion on mixed poly(dimethylaminoethyl methacrylate)/poly(acrylamidophenyl boronic acid)

brush surfaces, Langmuir, 31 (44) (2015), pp. 12054-12060
[13] H. Liu, et al., Dual-responsive surfaces modified with phenylboronic acid-containing polymer brush to reversibly capture and release cancer cells, J. Am. Chem. Soc., 135 (20) (2013), pp. 7603-7609
[14] S. Elfeky, Novel bronic acid-based fluorescent sensor for sugars and nucleosides, Curr. Org. Synth., 8 (6) (2011), pp. 872-880
[15] R. Amin, S.A. Elfeky, Fluorescent sensor for bacterial recognition, Spectrochim. Acta A Mol. Biomol. Spectrosc., 108 (2013), pp. 338-341
[16] R. Wannapob, et al., Affinity sensor using 3-aminophenylboronic acid for bacteria detection, Biosens. Bioelectron., 26 (2) (2010), pp. 357-364
[17] A. Matsumoto, N. Sato, K. Kataoka, Y. Miyahara, Noninvasive sialic acid detection at cell membrane by using phenylboronic acid modified self-assembled monolayer gold electrode, J. Am. Chem. Soc., 131 (34) (2009), pp. 12022-12023
[18] J. Quirós, S. Gonzalo, B. Jalvo, K. Boltes, J.A. Perdigón-Melón, R. Rosal, Electrospun cellulose acetate composites containing supported metal nanoparticles for antifungal membranes, Sci. Total Environ., 563-564 (2016), pp. 912-920
[19] J. Choi, T. Konno, R. Matsuno, M. Takai, K. Ishihara, Surface immobilization of biocompatible phospholipid polymer multilayered hydrogel on titanium alloy, Colloids Surf. B: Biointerfaces, 67 (2) (2008), pp. 216-223
[20] K. Shiomori, A.E. Ivanov, I.Y. Galaev, Y. Kawano, B. Mattiasson, Thermoresponsive properties of sugar sensitive copolymer of N-Isopropylacrylamide and 3-(Acrylamido)phenylboronic acid, Macromol. Chem. Phys., 205 (1) (2004), pp. 27-34
[21] G. Pasparakis, M. Vamvakaki, N. Krasnogor, C. Alexander, Diol-boronic acid complexes integrated by responsive polymers-a route to chemical sensing and logic operations, Soft Matter, 5 (20) (2009), pp. 3839-3841
[22] D. Roy, J.T. Guthrie, S. Perrier, Synthesis of natural-synthetic hybrid materials from cellulose via the RAFT process, Soft Matter, 4 (1) (2008), pp. 145-155
[23] S.H. Brewer, et al., Infrared detection of a phenylboronic acid terminated alkane thiol monolayer on gold surfaces, Langmuir, 20 (13) (2004), pp. 5512-5520
[24] J. Quirós, K. Boltes, R. Rosal, Bioactive applications for electrospun fibers, Polym. Rev., 56 (4) (2016), pp. 631-667
[25] M.C. van Loosdrecht, W. Norde, A.J. Zehnder, Physical chemical description of bacterial adhesion, J. Biomater. Appl., 5 (2) (1990), pp. 91-106
[26] J. Drelich, E. Chibowski, D.D. Meng, K. Terpilowski, Hydrophilic and superhydrophilic surfaces and materials, Soft Matter, 7 (21) (2011), pp. 9804-9828
[27] B. Gottenbos, D.W. Grijpma, H.C. van der Mei, J. Feijen, H.J. Busscher, Antimicrobial effects of positively charged surfaces on adhering Gram-positive and Gram-negative bacteria, J. Antimicrob. Chemother., 48 (1) (2001), pp. 7-13
[28] S. Halder, et al., Alteration of Zeta potential and membrane permeability in bacteria: a study with cationic agents, Springerplus, 4 (2015), p. 672
[29] G. Neumann, et al., Energetics and surface properties of *Pseudomonas putida* DOT-T1E in a two-phase fermentation system with 1-decanol as second phase, Appl. Environ. Microbiol., 72 (6) (2006), pp. 4232-4238
[30] J. Santiago-Morales, G. Amariei, P. Letón, R. Rosal, Antimicrobial activity of poly(vinyl alcohol)-poly(acrylic acid) electrospun nanofibers, Colloids Surf. B: Biointerfaces, 146 (2016), pp. 144-151
[31] L.A. Goetz, B. Jalvo, R. Rosal, A.P. Mathew, Superhydrophilic anti-fouling electrospun cellulose acetate membranes coated with chitin nanocrystals for water filtration, J. Membr. Sci., 510 (2016), pp. 238-248
[32] B. Jalvo, J. Santiago-Morales, P. Romero, R. Guzman de Villoria, R. Rosal, Microbial colonisation of transparent glass-like carbon films triggered by a reversible radiation-induced hydrophobic to hydrophilic transition, RSC Adv., 6 (55) (2016), pp. 50278-50287
[33] B. Wang, Y. Zhang, L. Shi, J. Li, Z.Y. Guo, Advances in the theory of superhydrophobic surfaces, J. Mater. Chem., 38 (2012), pp. 20112-20127
[34] K. Berggren, et al., Background-free, high sensitivity staining of proteins in one- and two-dimensional sodium dodecyl sulfate-polyacrylamide gels using a luminescent ruthenium complex, Electrophoresis, 21 (12) (2000), pp. 2509-2521
[35] S.-J. Chen, J.-F. Chang, N.-J. Cheng, J.-N. Yih, K.-C. Chiu, Detection of saccharides with a fluorescent sensing device based on a gold film modified with 4-mercaptophenylboronic acid monolayer, SPIE Proceedings 8812 (2013), pp. 881210-881219
[36] S. Liu, et al., Affinity interactions between Phenylboronic acid-carrying self-assembled monolayers and Flavin adenine dinucleotide or horseradish peroxidase, Chem. Eur. J., 11 (14) (2005), pp. 4239-4246
[37] Y. Okasaka, H. Kitano, Direct spectroscopic observation of binding of sugars to polymers having phenylboronic acids substituted with an ortho-phenylazo group, Colloids Surf. B: Biointerfaces, 79 (2) (2010), pp. 434-439
[38] L. Brown, J.M. Wolf, R. Prados-Rosales, A. Casadevall, Through the wall: extracellular vesicles in Gram-positive bacteria, mycobacteria and fungi, Nat. Rev. Microbiol., 13 (10) (Oct 2015), pp. 620-630
[39] B. Fournier, D.J. Philpott, Recognition of Staphylococcus aureus by the innate immune system, Clin. Microbiol. Rev., 18 (3) (2005), pp. 521-540
[40] K. Lacina, P. Skládal, T.D. JamesBoronic acids for sensing and other applications - A mini-review of papers published in 2013, Chem. Cent. J., 8 (1) (2014), p. 60

SUPPLEMENTARY DATA

Electrospun boronic acid-containing polymer membranes as fluorescent sensors for bacteria detection

Jennifer Quirós[a,b], Adérito J. R. Amaral[b] George Pasparakis[b], Gareth R. Williams[b], Roberto Rosal[a].

[a] *Department of Chemical Engineering, University of Alcalá, 28871 Alcalá de Henares, Madrid, Spain*

[b] *UCL School of Pharmacy, University College London, 29-39 Brunswick Square, London WC1N 1AX,U.K.*

Contents:

Table S1 Water contact angles of polymeric films. Microscope cover glasses (13 mm diameter) were coated with polymer blends at the same ratios of those of the fibers and dried at 50 ºC for 24 h.

Sample Name	Water Contact Angle (°)
PAN	56 ± 4
pVDB40@PAN	83 ± 5
pVDB50@PAN	85 ± 3
pVDB60@PAN	87 ± 3

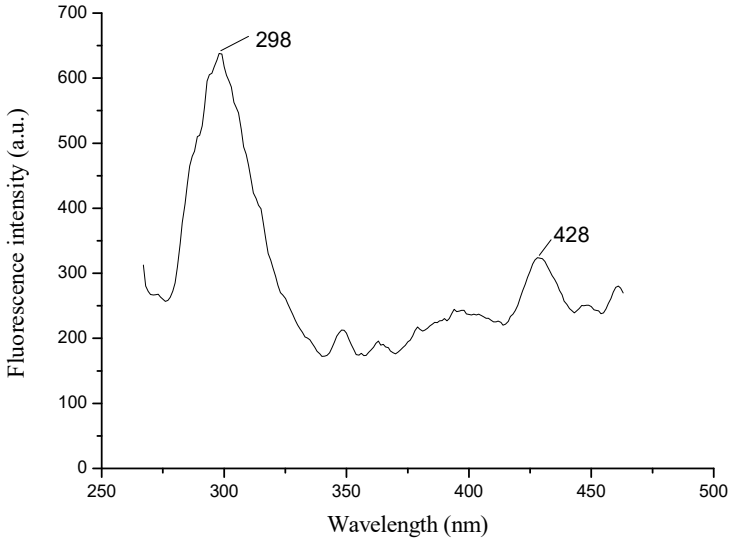

Fig. S1 The fluorescence spectrum of pVDB60@PAN (Λ_{ex} = 255 nm).

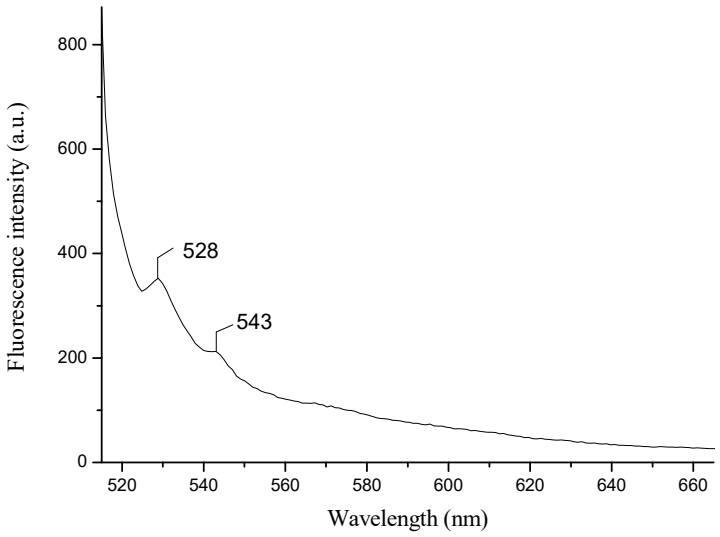

Fig. S2 The fluorescence spectrum of pVDB60@PAN (Λ_{ex} = 505 nm)

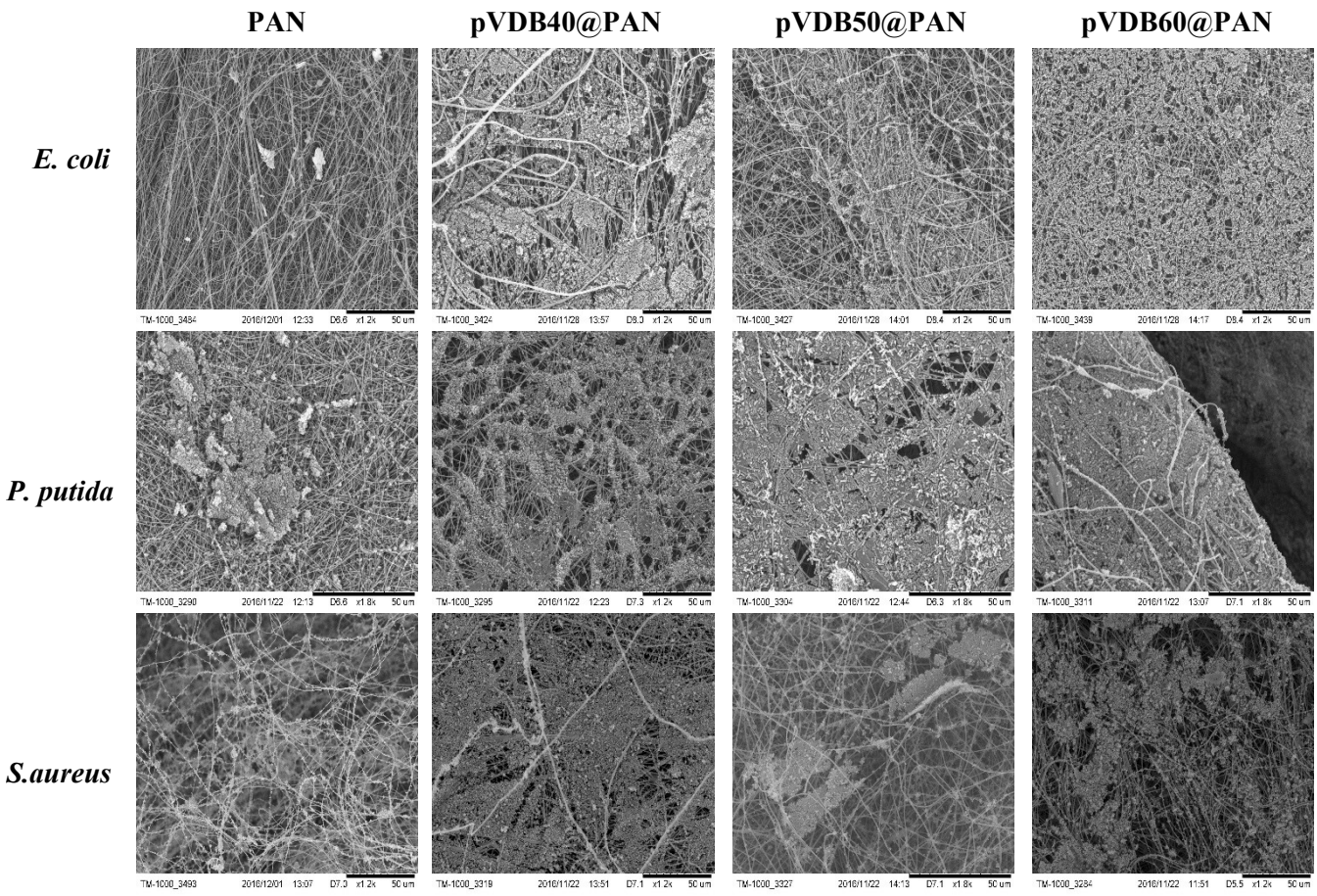

Fig. S3 SEM micrographs of PAN, pVDB40@PAN, pVDB50@PAN and pVDB60@PAN membranes after 48 h in contact with cultures of *E. coli*, *S. aureus* and *P. putida* (at 28 ºC for *P. putida* or 30 ºC for *S. aureus* and *E. coli*). Scale bars = 50 μm.

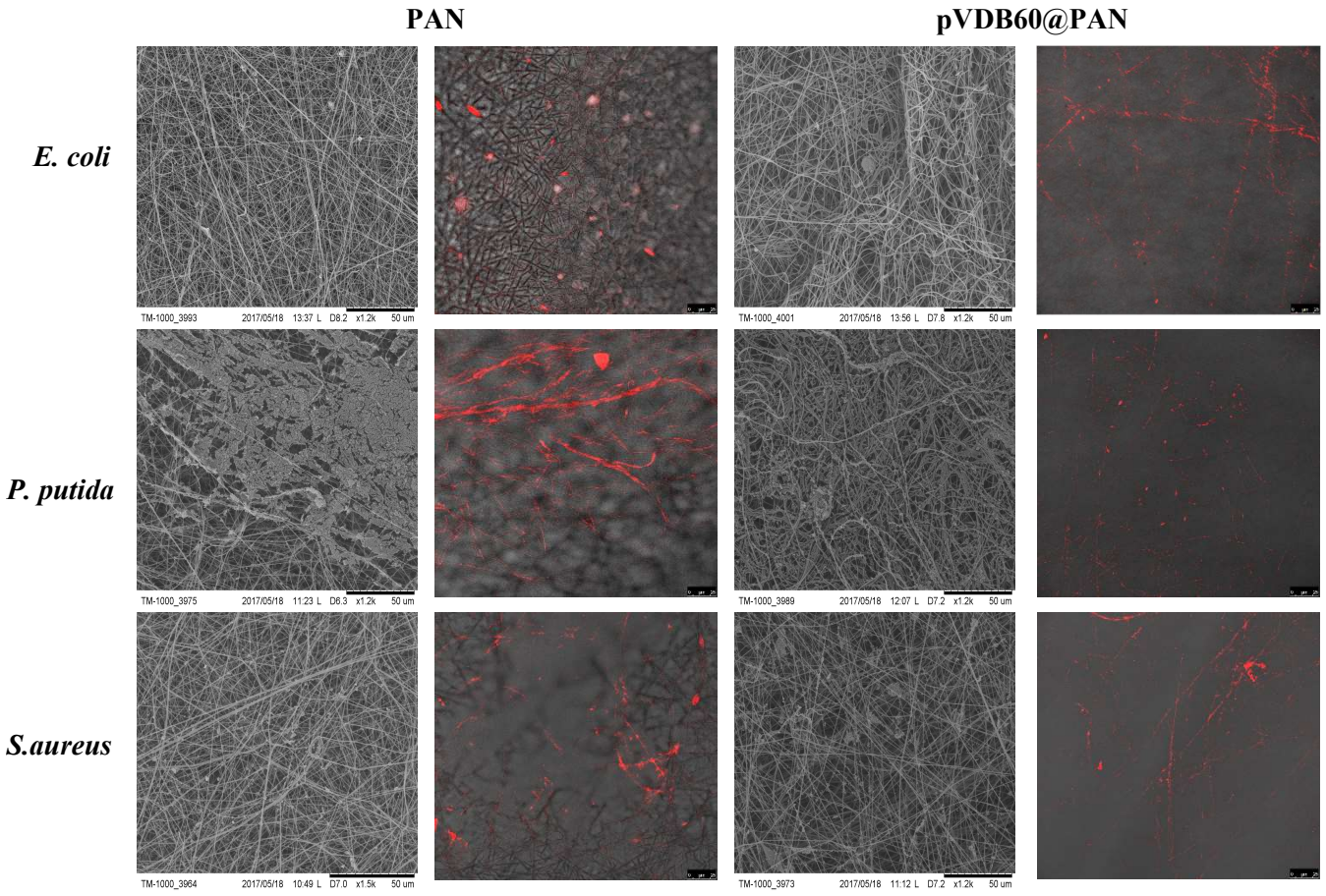

Fig. S4 SEM (scale bars = 50 μm) and confocal micrographs (scale bars = 25 μm) of PAN, pVDB40@PAN, pVDB50@PAN and pVDB60@PAN membranes after 6 h in contact with 1 g/L of glucose (extracted before cultures were added), and then 24 h with cultures of *E. coli*, *S. aureus* and *P. putida* (at 28 ºC for *P. putida* or 30 ºC for *S. aureus* and *E. coli*).